Calcium Entry-Calcium Refilling (CECR) coupling between store-operated Ca^{2+} entry and sarco/endoplasmic reticulum Ca^{2+}-ATPase

Isabel M. Manjarrés, María Teresa Alonso and Javier García-Sancho*

From Instituto de Biología y Genética Molecular (IBGM), Universidad de Valladolid y Consejo Superior de Investigaciones Científicas (CSIC), c/ Sanz y Forés 3, 47003 Valladolid, Spain.

***Corresponding Author:** Dr. J. García-Sancho, IBGM, c/Sanz y Forés 3, 47003-Valladolid, Spain. Phone: 34-983-423084; Fax: 34-983-421800; e.mail: jgsancho@ibgm.uva.es

ABSTRACT

Cross-talk between subcellular organelles is essential for cellular Ca^{2+} homeostasis. We have studied the effects of knocking down STIM1, the Ca^{2+} sensor of the endoplasmic reticulum (ER), on several homeostatic Ca^{2+}-handling mechanisms, including plasma membrane Ca^{2+} entry and transport by ER, mitochondria and nucleus. We have used targeted aequorins to selectively measure calcium fluxes in different organelles. Actions of STIM1 were extremely selective, restricted to store operated Ca^{2+} channels (SOC) and Ca^{2+} uptake by the ER. No interactions with uptake or release of Ca^{2+} by mitochondria or nucleus were detected. Ca^{2+} exit from the ER, including passive leak, release via inositol 1,4,5-trisphosphate and ryanodine receptors, was unaffected. STIM1 knock-down inhibited ER Ca^{2+} uptake in intact but not in permeabilized cells, suggesting a privileged calcium entry-calcium refilling (CECR) coupling between plasma membrane SOC and ER calcium pump in the intact cell. As a result a large part of the entering Ca^{2+} is taken up into the ER without reaching the bulk cytosol. The tightness of CECR, as measured by the slope of the stimulus-signal strength function, was comparable to classic excitation-response coupling mechanisms, such as excitation-contraction, excitation-secretion or excitation-transduction coupling.

1. Introduction

Changes of the cytosolic free Ca^{2+} concentration ($[Ca^{2+}]_C$) are key activation signals for many physiological processes. Subcellular compartmentation in different Ca^{2+} pools and cross-talk between them are essential for generation of high $[Ca^{2+}]_C$ microdomains and modulation of the messages [1]. Ca^{2+} release from the endoplasmic reticulum (ER), which can be triggered by a variety of intracellular messengers, is one of the main mechanisms for generation of $[Ca^{2+}]_C$ signals. The signal produced by Ca^{2+} release can be amplified or prolonged in time by Ca^{2+} entry from the extracellular medium through plasma membrane Ca^{2+} channels (store-operated Ca^{2+} channels, SOC). SOC opening is triggered directly by the emptying of the calcium stores (store-operated Ca^{2+} entry, SOCE) [2, 3]. The molecular identity of both the Ca^{2+} sensor that detects ER emptying, STIM1 [4], and the SOC channel, Orai1 [5], has been recently discovered and many molecular details on the transduction mechanism are now known [6, 7]. Activation of SOCE occurs by close interaction of STIM1 and Orai1 at a subplasmalemmal narrow space that comes very close to ER, the ER-plasma membrane junction [8]. Other proteins may associate to the STIM-Orai complexes [7, 9-11].

Apart from amplifying the Ca^{2+} signal, SOCE facilitates Ca^{2+} refilling of the ER after Ca^{2+} release [2, 3]. Putney initially proposed the name of Capacitative Calcium Entry (CCE) for this kind of ER refilling by analogy to charge accumulation by an electric capacitor [3]. Coupling between SOC and SERCA during activation of CCE is very tight and allows very efficient Ca^{2+} pumping into the stores [12-14]. Tight excitation-response (E-R) transduction is essential for many physiological functions. The idea was first developed for excitation-contraction (E-C) coupling in skeletal muscle [15] and then extended to synapse excitation-secretion (E-S) [16] and nucleus excitation-transcription (E-T) coupling [17]. This preferential coupling is characterized by a "*sharp threshold*" [15] that conditions a 10-fold increase in response (signal strength) to a 5-15 mV change in the stimulus. Coupling of SOCE to Ca^{2+}-handling by the different intracellular organelles could also be studied under this perspective.

Using the same elementary mechanisms as modules in different transduction systems is not uncommon in nature. It would not be surprising, therefore, that information on store-filling was relayed, apart from SOC, in other Ca^{2+}-handling mechanisms. It has been suggested for example that STIM1 could interact with other plasma membrane Ca^{2+} channels, such as TRP channels or ARC [6, 7, 11, 18]. Nevertheless, possible relationships of STIM1 with other intracellular Ca^{2+}-handling mechanisms essential for Ca^{2+} homeostasis have not been explored. Here we have used targeted aequorin probes to monitor Ca^{2+} transport in different organelles and have investigated the possible role of STIM1 by interfering with its expression using siRNA.

2. Materials and methods

2.1. DNA constructs

Fusion genes of wild type aequorin (AEQ) or its low Ca^{2+} affinity mutant (mutAEQ) to GFP (GA) and to different targeting sequences, such as ER (ermutGA), mitochondria (mitGA and mitmutGA) or nucleus (nucGA) were generated as previously described [19, 20]. The siRNA STIM1 sequence (AGAAGGAGCUAGAAUCUCACUU) and siRNA random sequence (AGGUAGUGUAAUCGCCUUGUU) were synthesized by MWG Biotech AG [21]. A red fluorescent marker siGLO OPTI-red (Thermo Scientific Dharmacon) was used in co-transfection with siRNA in some cases. Type 2 ryanodine receptor (RyR_2) cDNA was a kind gift of Dr. D.H. MacLennan, University of Toronto, Ontario, Canada.

2.2. Cell culture and transfection

HEK293T cells (ATCC CRL-11268) were cultured in DMEM supplemented with 10% fetal bovine serum, 100 U/ml penicillin, 100 µg/ml streptomycin and 2 mM glutamine under 5% CO_2 at 37 ºC. They were seeded in 35 mm wells at 5 x 10^5 cell/well and transfected one day later with 50-100 nM siRNA, 1 µg of GA cDNA, and, if necessary, 2 µg pcDNA3 RyR_2, using 10 µl of Lipofectamine 2000 (Invitrogen). The following day the cells were trypsinized and seeded again over poly-L-lysine coated 12 mm coverslips at 5 x 10^4 cells/coverslip for the fluorescence experiments or in 15 mm wells (7 x 10^4 cells/well) for bioluminescence experiments. Calcium measurements were performed 48-72 h after transfection.

2.3. Western blotting

Cells were seeded and transfected as described above. Extracts were prepared 48-72 h later by protein extraction with a cold lysis buffer of the following composition: 150 mM NaCl, 1 mM EDTA, 0.1 mM PMSF, 25 mM NaF, 5 mM Na_3VO_4, 1% NP-40, 100 µg/ml aprotinin, 100 µg/ml pepstatin, 100 µg/ml leupeptin A, 10 mM Tris-HCl, pH 8. Then 100 µg protein (estimated by BCA assay; Pierce) were separated by 8% PAGE. After electrotransfer of the membranes, the upper half (>75 kDa) was incubated overnight with a rabbit anti-STIM1 antibody (1:500; Alpha Diagnostic) and the lower half (<75 kDa) was incubated with a rabbit anti-actin antibody (1:1000; Sigma). Both membranes were treated then with a horseradish-peroxidase-labeled secondary antibody (1:2000; Bio-Rad) for 1h and bands were detected by chemiluminescence. Quantification of STIM1 expression was carried out using a GS-800 densitometer (BioRad).

2.4. Ca^{2+} imaging experiments

Measurements were performed in cells loaded with fura-2 or fluo-4 as described before [22, 23]. Briefly, cells were loaded by a 60 min incubation with 4 (fura-2) or 2 µM (fluo-4) of the corresponding acetoxymethyl esters (Molecular Probes) in a standard calcium-free solution containing (in mM): NaCl, 145; KCl,

5; $MgCl_2$, 1; glucose, 10; EGTA, 0.5; sodium-HEPES, 10, pH 7.4. Then the coverslips were mounted in a perfusion chamber under a 20x Olympus PlanApoUV objective in a Nikon Diaphot microscope. For fura-2 experiments, cells were alternately epi-illuminated at 340-380 nm and light emitted above 520 nm was recorded using a Hamamatsu Digital Camera C4742-98 handled by Simple PCI 6.6 Hamamatsu software. Consecutive frames obtained at 340 and 380 nm excitation were ratioed pixel by pixel using ImageJ software and calibrated in $[Ca^{2+}]_C$ by comparison with fura-2 standards. For fluo-4-loaded cells illumination was at 490 nm and results were expressed as F/F_0. Refilling of the Ca^{2+} stores was achieved by perfusion of a standard medium containing 1 mM $CaCl_2$ instead of EGTA.

2.5. Bioluminescence Ca^{2+} measurements

For $[Ca^{2+}]_{ER}$ measurements, cells transfected with ermutGA were incubated for 60 min in the dark with Ca^{2+}-free medium containing 1 μM coelenterazine n to allow reconstitution of AEQ. Coelenterazine n decreases further the sensitivity of AEQ for Ca^{2+} [24, 25]. In order to keep empty the intracellular Ca^{2+} stores, 10 μM 2,5-di*tert*-butyl-benzohidroquinone (TBH; Aldrich), a reversible SERCA inhibitor [26], was added to the medium. For Ca^{2+} measurements in nucleus or the mitochondria, AEQ wt was reconstituted by native coelenterazine (coel wt) in standard solution containing 1 mM $CaCl_2$. In some cases, other SERCA inhibitors, such as thapsigargin [27] or cyclopiazonic acid [28] (Bionova), were used to empty Ca^{2+} stores before or during the measurements. Cells were mounted in a superfusion chamber (3-5 ml/min) and luminescence was measured using a luminometer constructed under our design by Cairn Research Ltd. Data are primarily expressed as L/L_{TOTAL}, where L is the light output at a given moment and L_{TOTAL} is the sum of all the light counts remaining in the sample at that moment. The experiments were always terminated by perfusing with a solution containing 100 μM digitonin and 10 mM Ca^{2+} in order to release all the residual light counts. Calibrations in $[Ca^{2+}]$ were done using the values published before [29]. All the Ca^{2+} measurements were carried out at 22ºC. In experiments with permeabilized cells we used for perfusion an intracellular-like solution containing (in mM): KCl, 140; KH_2PO_4, 1; sodium succinate, 2; sodium pyruvate, 1; $MgCl_2$, 1; Mg-ATP, 1; sodium-HEPES, 20, pH 7.2; This medium was supplemented with EGTA or EGTA-Ca^{2+} buffers to achieve the desired $[Ca^{2+}]$ [30]. Caffeine, ATP, carbachol and digitonin were from Sigma. EGTA and inositol 1,4,5-trisphosphate (IP_3) were from Molecular Probes. Ionomycin was from SATO'S.

2.6. Statistics

Data are expressed as mean ± s.e.m. Significance levels (* $p<0.05$, ** $p<0.01$ and *** $p<0.001$) were estimated by t test for two groups of data (non-paired data) or ANOVA and Bonferroni test for three or more groups of data using GraphPad InStat software (San Diego, USA).

3. Results

3.1. ER takes up Ca^{2+} entering though SOCs very efficiently and slows down its passage to the bulk cytosol

We first studied the relationship between the Ca^{2+} entry through SOCE and the uptake into different organelles. Influx should be directly proportional to the extracellular Ca^{2+} concentration ($[Ca^{2+}]_E$), so that we measured Ca^{2+} transport into the different intracellular compartments at different $[Ca^{2+}]_E$ in the range between 0.1 and 10 mM. Fig. 1 summarizes the results. After emptying the intracellular Ca^{2+} stores by treatment with 10 μM TBH in Ca^{2+}-free medium for 60 min, we measured the initial rates of increase of $[Ca^{2+}]$ inside the different intracellular compartments (cytosol, nucleus, mitochondria and ER) at different $[Ca^{2+}]_E$. The results in nucleus and cytosol were similar, so that only nucleus has been shown in Fig. 1 for simplicity. The dependence of the rate of Ca^{2+} uptake on $[Ca^{2+}]_E$ was similar in nucleus and mitochondria. The slope of the lines in the double logarithmic representation of Fig. 1 was 0.30-0.32. This means that the rate of $\Delta[Ca^{2+}]$ inside these compartments raise about 2-fold by increasing 10 times $[Ca^{2+}]_E$. In the case of ER the dependence of the uptake on $[Ca^{2+}]_E$ was much steeper. The slope of the line was 1.76, indicating that the rate of $[Ca^{2+}]_{ER}$ increase produced by raising $[Ca^{2+}]_E$ was about 60-fold per decade.

On the overall, the dependence of Ca^{2+} uptake on $[Ca^{2+}]_E$ was 30 times steeper for the ER than for the other subcellular compartments studied. This output indicates that coupling between CCE and ER uptake is specially tight, in such a way that much of the Ca^{2+} entering into the cell though SOC goes directly to the ER without, apparently, reaching the bulk of the cytosol. The corollary to this interpretation is that preventing ER uptake should increase the $[Ca^{2+}]$ peak observed in the cytosol after activation of CCE. This prediction was confirmed by the results shown in Fig. 2, where the size of the Ca^{2+} overshoots produced by addition of extracellular Ca^{2+} to cells with emptied Ca^{2+} stores in the absence (first peak) and in the presence of TBH (second peak) were compared (Fig. 2A). The $\Delta[Ca^{2+}]_C$ was almost five fold larger in the second overshoot, suggesting that when SERCA action is not prevented by TBH much of the entering Ca^{2+} is taken up by the ER and does not reach the bulk cytosol. When TBH was present during the first Ca^{2+} overshoot, the size of the Ca^{2+} peak was similarly high (Fig. 2B). Finally, in another set of experiments thapsigargin, an irreversible SERCA inhibitor [27], also produced a large $\Delta[Ca^{2+}]_C$ (Fig. 2C). We conclude that, in intact cells, ER takes up a large fraction of the Ca^{2+} entering though active SOCs, thus hindering the increase of $[Ca^{2+}]_C$ in the bulk cytosol.

3.2. Knocking down STIM1 slows down Ca^{2+} uptake by the ER in intact HEK-293T cells.

STIM1 siRNA [21] decreased very much the expression of the endogenous STIM-1 in HEK-293T cells (Supplemental Fig. S1). Functional effects were assessed by measuring SOCE in cells co-transfected with STIM1 siRNA and the tracer siGLO red, used to identify the transfected cells. Fura-2-

loaded cells were treated with 1 μM thapsigargin for 7 min in Ca^{2+}-free medium and then they were challenged with 1 mM Ca^{2+} (Fig. 3). Changes in $[Ca^{2+}]_C$ were followed at the single-cell level. Cells were identified as positive (+siRNA) or negative (Control) by their red fluorescence and the averaged traces for each subpopulation were calculated. It is clear that the Ca^{2+} overshoot was smaller in the cells that had internalized the siRNA. The average values for $\Delta[Ca^{2+}]_C$ were (in nM; mean ± s.e.m.) 121 ± 25 in siRNA-transfected cells (n=16) *vs* 513 ± 95 in the control cells (n=10). This inhibition (75 %) was statistically significant ($p<0.001$).

Another set of experiments was designed for studying the effects of STIM1 siRNA on accumulation of Ca^{2+} by the ER. For these purposes, the cells were co-transfected with ermutGA and the STIM1 siRNA. The intracellular Ca^{2+} stores were depleted by treatment with the reversible SERCA inhibitor TBH (10 μM) for 60 min in a Ca^{2+}-free medium, and Ca^{2+} uptake was started by incubation with medium containing 1 mM Ca^{2+}. $[Ca^{2+}]_{ER}$ was measured directly by the aequorin luminescence. Results are show in Fig. 4A, where the outcome in control untreated cells, in cells treated with STIM1 siRNA and in cells treated with scrambled siRNA are compared. Scrambled siRNA did not modify the rate of Ca^{2+} uptake into the ER. On the contrary, STIM1 siRNA strongly decreased the rate of ER uptake. Fig. 4B compares the average values (mean ± s.e.m.) obtained in 8 similar experiments. The rate of ER uptake was not significantly modified by the scrambled siRNA but it was inhibited by 75 % by the STIM-1 siRNA ($p<0.001$).

3.3. STIM1 does not directly interact with the ER Ca^{2+}pump

In order to test whether STIM1 directly interacts with the ER Ca^{2+} pump, we studied the effects on ER Ca^{2+} uptake in permeabilized cells. For these experiments, control, untreated cells, and cells transfected with either STIM1 siRNA or scrambled siRNA were incubated with TBH to empty the intracellular Ca^{2+} stores as described above. The plasma membrane was then permeabilized by a brief treatment with digitonin and these cells were incubated with an intracellular-like medium containing different concentrations of Ca^{2+}, buffered with EGTA. The results are illustrated in Fig. 5. Panels A and B compare the uptake at a concentration range of 20-500 nM in control (A) and STIM1 siRNA-transfected cells (B). Parallel experiments performed with scrambled siRNA are not illustrated. Averaged values of several similar experiments are shown in Fig. 5C. It is clear that STIM had no effects on SERCA pumping in permeabilized cells. Overall, the activity had a V_{max} of about 29 μM/s, a K_{50} of about 150 nM and a Hill number of 2.8. These values are consistent with those reported previously for the SERCA2b isoform [31].

3.4. STIM1 does not affect either ER Ca^{2+} leak or Ca^{2+} release through either IP_3 receptors or ryanodine receptors

Next, we studied whether STIM1 could interact with the mechanisms responsible for Ca^{2+} exit from the intracellular calcium stores. STIM1 locates in the membrane of the ER, where the Ca^{2+} channels responsible for passive leak or receptor-induced release also lay. For this reason we formulated the working

hypothesis that interactions between these proteins could occur and have consequences in Ca^{2+} homeostasis. In order to test this hypothesis, we investigated the effects of decreasing STIM1 levels on these two Ca^{2+} transport mechanisms.

We studied passive leak in intact cells expressing ermutGA. For this purpose, the intracellular Ca^{2+} stores were allowed to refill and then external Ca^{2+} was removed and the decrease of $[Ca^{2+}]_{ER}$ as a function of time was followed. A typical experiment comparing control cells and cells transfected with either scrambled siRNA or STIM1 siRNA is shown in Fig. 6A. On removal of the external Ca^{2+} there was an slow decrease of $[Ca^{2+}]_{ER}$ reflecting leak from the ER. When represented in logarithmic scale the decrease of $[Ca^{2+}]_{ER}$ became linear with time, evidencing that the exit followed a single exponential model with a first order rate constant of about -0.002 s^{-1} (Supplemental Fig. S2A). The averaged results from 4 similar experiments of each type are shown in Fig. 6B. The rates of exit were not significantly different in any of the conditions.

A similar experimental design was used to study the effects of STIM1 removal on the IP_3-induced release of Ca^{2+} from the ER. In this case, release was triggered by maximal stimulation with IP_3-producing-agonists, which was accomplished by adding the effects of the two signaling pathways with supramaximal doses of agonists (100 μM ATP plus 100 μM carbachol). Results are shown in Fig. 6C. The stimulation produced a biphasic release of a large part of the ER calcium pool. The logarithmic plot (Supplemental Fig. S2B) showed that the release could be described by the addition of two exponentials. The first one corresponded to a first order rate constant of about -0.07 s^{-1}, lasted for only a few seconds and emptied about 25% of the whole Ca^{2+} pool. The second phase was slower (k value, about -0.01 s^{-1}), lasted for the whole stimulation period (60 s) and produced the release of about another 25% of the ER Ca^{2+} pool (Supplemental Fig. S2B). Fig. 6D summarizes the results of 4 similar experiments. The treatment with STIM1 siRNA did not provoke any significant effect on the release of Ca^{2+} from the ER induced by the IP_3-producing agonists, neither during the rapid release (Fig. 6D) or the slower one (results not shown).

The effects of STIM1 on the ER Ca^{2+} leak and on the IP_3-induced Ca^{2+} release was also studied in cells whose plasma membrane had been permeabilized with digitonin. Results are shown in Fig. 7. Cells transfected with ermutGA were depleted of calcium by treatment with TBH for 60 min in Ca^{2+}-free medium. Cells were then permeabilized by a brief treatment with digitonin and the stores were allowed to refill by incubation with an intracellular-like solution containing 100 nM Ca^{2+} (buffered with EGTA). After 3 min-refilling, Ca^{2+} was removed and the decrease in $[Ca^{2+}]_{ER}$ was followed by AEQ luminescence. On Ca^{2+} removal with 2 mM EGTA, there was a Ca^{2+} leak (Fig. 7A) that followed a single exponential corresponding to k=0.01 s^{-1} (Supplemental Fig. S2C). This rate was similar to the one observed when SERCA was inhibited with 10 μM TBH or 10 μM cyclopiazonic acid (CPA) instead of with Ca^{2+} removal (Supplemental Fig. S2C). On stimulation with IP_3 (5 μM) there was a much faster Ca^{2+} release in the permeabilized cells (Fig. 7B). The fast release had a first order rate constant of about 0.07 s^{-1} (Supplemental Fig. S2C), similar

to the value estimated in intact cells (see above, Fig. 6C; Supplemental Fig. S2B). Blocking STIM1 with siRNA had no effect on Ca^{2+} leak from the ER nor on the IP_3 induced release (Fig7A, B and C).

We also studied the effects of STIM1 on Ca^{2+} efflux from the ER through ryanodine receptors (RyR). RyR2 was overexpressed in HEK293T cells to maximize transport though this mechanism. Cells were co-transfected with RyR_2 and ermutGA at a DNA ratio of 2:1 in order to be sure that the cells expressing the aequorin also expressed the RyR. A summary of the results is shown in Fig. 8. For the experiments in intact cells, ER was depleted by treatment with TBH in Ca^{2+}-free medium and then refilled by incubation with Ca^{2+} as in Fig. 4. Different concentrations of caffeine were used to induce release at different filling periods. The protocol is illustrated by two typical experiments in Supplemental Fig. S3A and S3B, where the results obtained in controls and in cells treated with STIM1 siRNA are compared. The regulation of release through RyR is complex, as it depends on both of the concentration of caffeine and the Ca^{2+} content of the ER [32]. We tested the effects of several caffeine concentrations ranging between 2 and 50 mM and several $[Ca^{2+}]_{ER}$ levels, from below 200 to above 2000 μM. Results are summarized in Fig 8A, where we have plotted the rates of Ca^{2+} release form ER against the initial $[Ca^{2+}]_{ER}$ level and fitted to straight lines grouping each caffeine concentration. From these data, the facilitating action of both caffeine and the $[Ca^{2+}]_{ER}$ level becomes evident, although the controls and cells with knocked-down STIM1 behaved similarly.

Experiments with caffeine were also performed in permeabilized cells where the degree of ER refilling could be controlled precisely by incubation with different $[Ca^{2+}]_C$ concentrations (Ca^{2+} buffered with EGTA). Representative results comparing the effects of two caffeine concentrations in control and STIM1 siRNA-transfected cells are shown in Supplemental Fig. S4. Caffeine induced comparable releases in both cases. The same results were also obtained with other caffeine and $[Ca^{2+}]_{ER}$ concentrations (not shown). The rates of caffeine-induced release were very similar in intact and permeabilized cells. All the results have been grouped in the three-dimensional plot of Fig.8B. It is clear that Ca^{2+} release increases both with caffeine concentration and with $[Ca^{2+}]_{ER}$, but there is no difference in the distribution of controls (red and magenta) and STIM1 siRNA-transfected cells (dark and light blue).

3.5. STIM1 does not interfere with Ca^{2+} handling by mitochondria and nucleus

Mitochondria and ER are very closely related, both physically and functionally [1, 33-39]. They share much the same $[Ca^{2+}]_C$ microdomains [1, 35] and can recycle the Ca^{2+} released from one organelle into the other [23, 40-44] or even tunnel Ca^{2+} among different parts of the cell without passaging through the cytosol [45, 46]. Therefore, the existence of a cross-talk on Ca^{2+} handling between ER and mitochondria would not be unexpected. In this way, information on the filling degree of the ER, as it could be provided by STIM1, could be used for regulation of mitochondrial Ca^{2+} transport.

In a series of experiments we followed mitochondrial Ca^{2+} uptake in cells transfected with mitGA. When STIM1 expression was knocked down with the siRNA, mitochondrial uptake following activation of CCE was decreased (Supplemental Fig. S5). This could be due to either a decrease of Ca^{2+} entry through the plasma membrane (Fig. 3), or to an inhibition of mitochondrial transport mechanisms. In order to directly study mitochondrial transport we performed experiments in permeabilized cells, measuring mitochondrial calcium uptake at different $[Ca^{2+}]_C$. Results demonstrated that there were not direct interactions between STIM1 and the mitochondrial Ca^{2+} uptake mechanisms, as mitochondrial Ca^{2+} accumulation (measured in this case using mitmutGA in order to increase the measurable concentration range) was unmodified by the treatment with STIM1 siRNA (Fig. 9).

Mitochondrial uptake of the Ca^{2+} released from the ER was also studied in another series of experiments. For this purpose cells transfected with mitGA were stimulated to release stored Ca^{2+} either with the IP_3-producing agonists ATP or carbachol (Supplemental Fig. S6A and S6B) or with caffeine (Supplemental Fig. S6C). In all the cases the Ca^{2+} peaks did not differ in controls and cells treated with STIM1 siRNA, suggesting that mitochondrial transport (both uptake and release) was unmodified by STIM1 knockdown.

Finally the increase of $[Ca^{2+}]_N$ produced by ATP-induced calcium release from the intracellular calcium stores was measured with nucGA and compared in control and in cells treated with STIM1 siRNA (Supplemental Fig. S7). The nuclear peaks were identical in both cases indicating no interference of STIM1 knockdown with Ca^{2+} transport through the nuclear envelope.

4. Discussion

The interactions of STIM1, the sensor of $[Ca^{2+}]_{ER}$, with Orai1 and other proteins involved in activation of SOCs have received much attention in the last years [6, 7], but a systematic study on the interactions of STIM1 with other Ca^{2+}-handling mechanisms was missing. Combining STIM1 knockdown by siRNA [21] with the use of targeted aequorin probes offers the opportunity to perform selective measurements of Ca^{2+} transport by the different organelles [1, 20, 32, 47]. Homeostatic Ca^{2+}-handling mechanisms of different subcellular organelles are closely related each other and subjected to cross-talk. However, the only effects of STIM1 reduction on the Ca^{2+} transport mechanisms that we were able to evidence were extremely selective, restricted physically to plasma membrane SOC channels and functionally to the ER Ca^{2+} uptake by SERCA. Our treatment reduced STIM1 expression by >50% (Supplemental Fig. S1) and SOCE by >70% (Fig. 3B), but neither transport of Ca^{2+} from cytosol to nucleus (Supplemental Fig. S7) nor mitochondrial transport, including both uptake and release (Fig. 9; Supplemental Fig. S6), were affected. Interactions of SOCE with nuclear transport were not expected, as diffusion through the nuclear envelope seems dominated by diffusional mechanisms [48]. However, mitochondrial Ca^{2+} handling is very closely related to SOCE [2, 42] but, according to our results, it seems to be no control of STIM1 over mitochondrial transport.

By contrast, Ca^{2+} transport by the ER was deeply influenced by CCE. Knocking down STIM1 inhibited selectively Ca^{2+} uptake into the ER in intact cells (Fig. 4) with no effects on the different exit mechanisms: passive leak (Fig. 6C; Fig. 7B) or release via IP_3 receptors (Fig. 6B; Fig. 7B) or ryanodine receptors (Fig. 8, Supplemental Fig. S3). On the other hand, the inhibition of Ca^{2+} entry into the ER was not observed in permeabilized cells (Fig. 5), suggesting that it is a functional effect that depends on the spatial coupling between the plasma membrane Ca^{2+} channels and SERCA in the intact cell. We have recently proposed that SERCA is (together with STIM1 and Orai1) the third element of CCE, to which is tightly coupled thus favoring rapid Ca^{2+} pumping from the high Ca^{2+} microdomains, generated at the SOC's mouth to the ER [13]. Therefore, the results in the present work reinforce previous proposals of a preferential coupling between ER and SOCE [9, 12-14] with biophysical arguments. Thus, acceleration of entry through the plasma membrane affected much more the rate of uptake into the ER than into the bulk cytosol itself, into the nucleus or into the mitochondria (Fig. 1). The idea is reminiscent of the original proposal of Putney [3], where Ca^{2+} was able to enter directly from the extracellular medium into the ER, bypassing the cytosol. Results in Fig. 2 indicate that only about 20% of all the calcium entering the cell during activation of SOCE reaches the bulk cytosol. The other 80% is accumulated into the ER, as blocking SERCA with thapsigargin or other inhibitors increases the size of the $[Ca^{2+}]_C$ peak by more than 5-fold. We propose the term "calcium entry-calcium refilling" (CECR) coupling to describe the very tight coupling shown here, which reminds the classic excitation-response (E-R) coupling mechanisms [15-17, 49]. In these cases the slope of the response-stimulus function was very steep determining a "*sharp threshold*" [15] that approaches the E-R relation to an "all or none" process. For example, the change in the stimulus required to increase the signal strength ten times

was of only 6 mV for skeletal muscle E-C coupling and 18 mV for heart E-C coupling (Table 1). In the case of CECR (Fig. 1) the steepness was similar: an 18 mV change in the stimulus was required for 10 fold increase of signal strength (Table 1). The remarkable preservation of ER refilling even at low STIM1 levels [12] could conceptually be explained as a manifestation of this all or none-like response. Several factors may contribute to do the threshold for ER refilling so sharp. First, the close proximity of the SOC channels to the ER pumps, as illustrated by the fact that permeabilization of the plasma membrane produces uncoupling by disturbing the spatial relationship between SOC and SERCA. Second, the fact that dependence of ER Ca^{2+} uptake on Ca^{2+} concentration is also very steep, with a Hill number of 2.8 (Fig. 5), helps to achieve the tight coupling as well.

Several studies have reported that mitochondrial function is required for activation of SOCE [2, 39]. However, mitochondria do not to localize near the STIM1 puncta [36, 39] and seem not to sense high $[Ca^{2+}]_C$ microdomains generated by activation of SOC [37, 38]. In the present study, we find almost no mitochondrial Ca^{2+} uptake is seen on activation of SOCs (Fig. 1). In contrast, we have earlier shown that activation of plasma membrane voltage-gated Ca^{2+} channels in chromaffin cells induces a large Ca^{2+} uptake into mitochondria [23, 29]. What is the reason for this difference? Comparing the kinetics of Ca^{2+} uptake by the ER (Fig. 5C) and by mitochondria (Fig. 9) as a function of $[Ca^{2+}]_C$ clarifies this point. In the intact cells, mitochondrial uptake reaches about $2 \cdot 10^{-6}$ M/s (Fig. 1); in permeabilized cells this mitochondrial uptake, less than 10 % of maximum, is attained with only 1-2 μM $[Ca^{2+}]_C$ (Fig. 9). At this concentration (Fig. 5C) Ca^{2+} uptake by the ER is maximum, about $3 \cdot 10^{-5}$ M, a value that is consistent with the maximum measured in the intact cells (Fig. 1). Therefore, the results found, with larger uptake by the ER than by mitochondria, are consistent with $[Ca^{2+}]_C$ microdomains of about 1 μM during activation of SOC mediated influx in HEK cells. In the case of chromaffin cells we have estimated that opening of the plasma membrane voltage-gated Ca^{2+} channels could generate $[Ca^{2+}]_C$ microdomains approaching 50 μM at the cytosol surrounding the mitochondria closer to the mouth of the channels [23, 29]. Under these conditions mitochondrial uptake predominates over ER accumulation, as mitochondrial V_{max} is about ten times larger (compare Fig. 5 and Fig. 9). This discrepant behavior also illustrates that different plasma membrane Ca^{2+} channels can generate high Ca^{2+} microdomains of various amplitudes, much larger in the case of voltage-gated channels than in the case of SOCs. Alternatively, SOCs could be relatively closer to ER and voltage-gated channels closer to mitochondria. Recent studies suggest that mitochondria are not specially close to STIM1 clusters [36, 38, 39]. We still have much to learn about functional consequences of organelle topology, but new and powerful techniques for molecular approach and visualization are now available [10]. On the other hand, the membrane of both organelles, ER and mitochondria, is extremely dynamic and can change very quickly both, in shape and closeness to the plasma membrane [42, 50].

Conflict of interests

None.

Acknowledgements

This work was supported by a grant from The Spanish Ministerio de Ciencia e Innovación (MICINN; grants BFI2007-60157; BFU2010-17379 and SAF2008-03175-E). IMM was supported by a fellowship from MICINN. We thank Dr. David H. MacLennan, University of Toronto, Toronto, Ontario, Canada for the RyR2 cDNA. Technical support from Miriam Garcia Cubillas is gratefully acknowledged.

References

1. Alonso MT, Villalobos C, Chamero P, Alvarez J, Garcia-Sancho J. (2006) Calcium microdomains in mitochondria and nucleus. Cell Calcium, 40, 513-25.
2. Parekh AB, Putney JW, Jr. (2005) Store-operated calcium channels. Physiol Rev, 85, 757-810.
3. Putney JW, Jr. (1986) A model for receptor-regulated calcium entry. Cell Calcium, 7, 1-12.
4. Roos J, DiGregorio PJ, Yeromin AV, Ohlsen K, Lioudyno M, Zhang S, Safrina O, Kozak JA, Wagner SL, Cahalan MD, Velicelebi G, Stauderman KA. (2005) STIM1, an essential and conserved component of store-operated Ca2+ channel function. J Cell Biol, 169, 435-45.
5. Feske S, Gwack Y, Prakriya M, Srikanth S, Puppel SH, Tanasa B, Hogan PG, Lewis RS, Daly M, Rao A. (2006) A mutation in Orai1 causes immune deficiency by abrogating CRAC channel function. Nature, 441, 179-85.
6. Clapham DE. (2009) A STIMulus Package puts orai calcium channels to work. Cell, 136, 814-6.
7. Cahalan MD. (2009) STIMulating store-operated Ca(2+) entry. Nat Cell Biol, 11, 669-77.
8. Wu MM, Buchanan J, Luik RM, Lewis RS. (2006) Ca2+ store depletion causes STIM1 to accumulate in ER regions closely associated with the plasma membrane. J Cell Biol, 174, 803-13.
9. Vaca L. (2010) SOCIC: the store-operated calcium influx complex. Cell Calcium, 47, 199-209.
10. Varnai P, Toth B, Toth DJ, Hunyady L, Balla T. (2007) Visualization and manipulation of plasma membrane-endoplasmic reticulum contact sites indicates the presence of additional molecular components within the STIM1-Orai1 Complex. J Biol Chem, 282, 29678-90.
11. Ong HL, Cheng KT, Liu X, Bandyopadhyay BC, Paria BC, Soboloff J, Pani B, Gwack Y, Srikanth S, Singh BB, Gill DL, Ambudkar IS. (2007) Dynamic assembly of TRPC1-STIM1-Orai1 ternary complex is involved in store-operated calcium influx. Evidence for similarities in store-operated and calcium release-activated calcium channel components. J Biol Chem, 282, 9105-16.
12. Jousset H, Frieden M, Demaurex N. (2007) STIM1 knockdown reveals that store-operated Ca2+ channels located close to sarco/endoplasmic Ca2+ ATPases (SERCA) pumps silently refill the endoplasmic reticulum. J Biol Chem, 282, 11456-64.
13. Manjarres IM, Rodriguez-Garcia A, Alonso MT, Garcia-Sancho J. (2010) The sarco/endoplasmic reticulum Ca(2+) ATPase (SERCA) is the third element in capacitative calcium entry. Cell Calcium, 47, 412-8.

14. Sampieri A, Zepeda A, Asanov A, Vaca L. (2009) Visualizing the store-operated channel complex assembly in real time: identification of SERCA2 as a new member. Cell Calcium, 45, 439-46.

15. Hodgkin AL, Horowicz P. (1960) Potassium contractures in single muscle fibres. J Physiol, 153, 386-403.

16. Katz B, Miledi R. (1967) The timing of calcium action during neuromuscular transmission. J Physiol, 189, 535-44.

17. Wheeler DG, Barrett CF, Groth RD, Safa P, Tsien RW. (2008) CaMKII locally encodes L-type channel activity to signal to nuclear CREB in excitation-transcription coupling. J Cell Biol, 183, 849-63.

18. Cahalan MD, Zhang SL, Yeromin AV, Ohlsen K, Roos J, Stauderman KA. (2007) Molecular basis of the CRAC channel. Cell Calcium, 42, 133-44.

19. Montero M, Brini M, Marsault R, Alvarez J, Sitia R, Pozzan T, Rizzuto R. (1995) Monitoring dynamic changes in free Ca2+ concentration in the endoplasmic reticulum of intact cells. EMBO J, 14, 5467-75.

20. Manjarres IM, Chamero P, Domingo B, Molina F, Llopis J, Alonso MT, Garcia-Sancho J. (2008) Red and green aequorins for simultaneous monitoring of Ca2+ signals from two different organelles. Pflugers Arch, 455, 961-70.

21. Mercer JC, Dehaven WI, Smyth JT, Wedel B, Boyles RR, Bird GS, Putney JW, Jr. (2006) Large store-operated calcium selective currents due to co-expression of Orai1 or Orai2 with the intracellular calcium sensor, Stim1. J Biol Chem, 281, 24979-90.

22. Villalobos C, Nunez L, Garcia-Sancho J. (1996) Functional glutamate receptors in a subpopulation of anterior pituitary cells. FASEB J, 10, 654-60.

23. Villalobos C, Nunez L, Montero M, Garcia AG, Alonso MT, Chamero P, Alvarez J, Garcia-Sancho J. (2002) Redistribution of Ca2+ among cytosol and organella during stimulation of bovine chromaffin cells. FASEB J, 16, 343-53.

24. Shimomura O, Musicki B, Kishi Y, Inouye S. (1993) Light-emitting properties of recombinant semi-synthetic aequorins and recombinant fluorescein-conjugated aequorin for measuring cellular calcium. Cell Calcium, 14, 373-8.

25. Barrero MJ, Montero M, Alvarez J. (1997) Dynamics of [Ca2+] in the endoplasmic reticulum and cytoplasm of intact HeLa cells. A comparative study. J Biol Chem, 272, 27694-9.

26. Moore GA, Kass GE, Duddy SK, Farrell GC, Llopis J, Orrenius S. (1990) 2,5-Di(tert-butyl)-1,4-benzohydroquinone--a novel mobilizer of the inositol 1,4,5-trisphosphate-sensitive Ca2+ pool. Free Radic Res Commun, 8, 337-45.

27. Thastrup O, Cullen PJ, Drobak BK, Hanley MR, Dawson AP. (1990) Thapsigargin, a tumor promoter, discharges intracellular Ca2+ stores by

specific inhibition of the endoplasmic reticulum Ca2(+)-ATPase. Proc Natl Acad Sci U S A, 87, 2466-70.

28. Seidler NW, Jona I, Vegh M, Martonosi A. (1989) Cyclopiazonic acid is a specific inhibitor of the Ca2+-ATPase of sarcoplasmic reticulum. J Biol Chem, 264, 17816-23.

29. Montero M, Alonso MT, Carnicero E, Cuchillo-Ibanez I, Albillos A, Garcia AG, Garcia-Sancho J, Alvarez J. (2000) Chromaffin-cell stimulation triggers fast millimolar mitochondrial Ca2+ transients that modulate secretion. Nat Cell Biol, 2, 57-61.

30. Bers DM, Patton CW, Nuccitelli R. (1994) A practical guide to the preparation of Ca2+ buffers. Methods Cell Biol, 40, 3-29.

31. Chandrasekera PC, Kargacin ME, Deans JP, Lytton J. (2009) Determination of apparent calcium affinity for endogenously expressed human sarco(endo)plasmic reticulum calcium-ATPase isoform SERCA3. Am J Physiol Cell Physiol, 296, C1105-14.

32. Alonso MT, Barrero MJ, Michelena P, Carnicero E, Cuchillo I, Garcia AG, Garcia-Sancho J, Montero M, Alvarez J. (1999) Ca2+-induced Ca2+ release in chromaffin cells seen from inside the ER with targeted aequorin. J Cell Biol, 144, 241-54.

33. Rizzuto R, Marchi S, Bonora M, Aguiari P, Bononi A, De Stefani D, Giorgi C, Leo S, Rimessi A, Siviero R, Zecchini E, Pinton P. (2009) Ca(2+) transfer from the ER to mitochondria: When, how and why. Biochim Biophys Acta.

34. Rizzuto R, Pinton P, Carrington W, Fay FS, Fogarty KE, Lifshitz LM, Tuft RA, Pozzan T. (1998) Close contacts with the endoplasmic reticulum as determinants of mitochondrial Ca2+ responses. Science, 280, 1763-6.

35. Rizzuto R, Pozzan T. (2006) Microdomains of intracellular Ca2+: molecular determinants and functional consequences. Physiol Rev, 86, 369-408.

36. Csordas G, Varnai P, Golenar T, Roy S, Purkins G, Schneider TG, Balla T, Hajnoczky G. (2010) Imaging interorganelle contacts and local calcium dynamics at the ER-mitochondrial interface. Mol Cell, 39, 121-32.

37. Giacomello M, Drago I, Bortolozzi M, Scorzeto M, Gianelle A, Pizzo P, Pozzan T. (2010) Ca2+ hot spots on the mitochondrial surface are generated by Ca2+ mobilization from stores, but not by activation of store-operated Ca2+ channels. Mol Cell, 38, 280-90.

38. Korzeniowski MK, Szanda G, Balla T, Spat A. (2009) Store-operated Ca2+ influx and subplasmalemmal mitochondria. Cell Calcium, 46, 49-55.

39. Naghdi S, Waldeck-Weiermair M, Fertschai I, Poteser M, Graier WF, Malli R. (2010) Mitochondrial Ca2+ uptake and not mitochondrial motility is required for STIM1-Orai1-dependent store-operated Ca2+ entry. J Cell Sci, 123, 2553-64.

40. Garcia AG, Garcia-De-Diego AM, Gandia L, Borges R, Garcia-Sancho J. (2006) Calcium signaling and exocytosis in adrenal chromaffin cells. Physiol Rev, 86, 1093-131.

41. Arnaudeau S, Kelley WL, Walsh JV, Jr., Demaurex N. (2001) Mitochondria recycle Ca(2+) to the endoplasmic reticulum and prevent the depletion of neighboring endoplasmic reticulum regions. J Biol Chem, 276, 29430-9.

42. Demaurex N, Poburko D, Frieden M. (2009) Regulation of plasma membrane calcium fluxes by mitochondria. Biochim Biophys Acta, 1787, 1383-94.

43. Filippin L, Magalhaes PJ, Di Benedetto G, Colella M, Pozzan T. (2003) Stable interactions between mitochondria and endoplasmic reticulum allow rapid accumulation of calcium in a subpopulation of mitochondria. J Biol Chem, 278, 39224-34.

44. Malli R, Frieden M, Trenker M, Graier WF. (2005) The role of mitochondria for Ca2+ refilling of the endoplasmic reticulum. J Biol Chem, 280, 12114-22.

45. Frieden M, Arnaudeau S, Castelbou C, Demaurex N. (2005) Subplasmalemmal mitochondria modulate the activity of plasma membrane Ca2+-ATPases. J Biol Chem, 280, 43198-208.

46. Mogami H, Nakano K, Tepikin AV, Petersen OH. (1997) Ca2+ flow via tunnels in polarized cells: recharging of apical Ca2+ stores by focal Ca2+ entry through basal membrane patch. Cell, 88, 49-55.

47. Alonso MT, Barrero MJ, Carnicero E, Montero M, Garcia-Sancho J, Alvarez J. (1998) Functional measurements of [Ca2+] in the endoplasmic reticulum using a herpes virus to deliver targeted aequorin. Cell Calcium, 24, 87-96.

48. Chamero P, Villalobos C, Alonso MT, Garcia-Sancho J. (2002) Dampening of cytosolic Ca2+ oscillations on propagation to nucleus. J Biol Chem, 277, 50226-9.

49. Chapman RA, Tunstall J. (1981) The tension-depolarization relationship of frog atrial trabeculae as determined by potassium contractures. J Physiol, 310, 97-115.

50. Orci L, Ravazzola M, Le Coadic M, Shen WW, Demaurex N, Cosson P. (2009) From the Cover: STIM1-induced precortical and cortical subdomains of the endoplasmic reticulum. Proc Natl Acad Sci U S A, 106, 19358-62.

TABLE 1. Comparison of the efficiency of excitation-response (E-R) coupling in different physiological systems. The value of the E/R relation was estimated from a plot of the response (signal strength), in log scale, *vs* stimulus (in mV). The slope was estimated in mV/decade increase of response. This value is inversely proportional to the efficiency of coupling. In the case of CECR, an equivalence of 30 mV per decade of Ca^{2+} concentration was assumed for the calculations.

	E-C (muscle)	**E-C (heart)**	**E-S (synapse)**	**E-T (nucleus)**	**CECR (This study)**
E/R in mV/decade	6	18	17	12	18
Reference	[15]	[49]	[16]	[17]	Fig. 1

Figure captions

Fig. 1. Kinetics of Ca^{2+} uptake into different organelles. Cells were transfected with either ermutGA, mitmutGA or nucGA. To study Ca^{2+} entry in intact cells, they were pre-treated with 10 μM TBH for 60 min in Ca^{2+}-free medium. After washing TBH for 1 min. in Ca^{2+}-free medium, then Ca^{2+} stores were allowed to refill by incubation with a standard solution containing 0.1, 0.3, 1, 3 and 10 mM Ca^{2+} and the initial rates of Ca^{2+} uptake were measured. Means ± s.e.m. from 19-38 independent experiments are shown. The measurements were performed with mutAEQ and coelenterazine n (ER and mitochondria) or with wild type AEQ and native coelenterazine (nucleus).

Fig. 2. Uptake into ER prevents the increase of $[Ca^{2+}]_C$ caused by SOCE. Cells loaded with fluo-4 in a Ca^{2+}-free solution containing 10 μM TBH were challenged with Ca^{2+}-containing medium (Ca1) to induce SOCE as shown. Cytosolic Ca^{2+} is expressed as F/F_0 (fluorescence excited at 490 nm and measured at 535 nm). **A**, after 5 min with Ca^{2+}, cells were transferred again to medium containing no Ca^{2+} and 10 μM TBH to re-empty the intracellular Ca^{2+} stores (Ca0+TBH) and then challenged with medium containing Ca^{2+} and 10 μM TBH to prevent ER refilling (Ca1+TBH). **B,** cells with empty stores were directly challenged with medium containing Ca^{2+} and 10 μM TBH. **C,** cells treated with the irreversible SERCA inhibitor thapsigargin (1 μM) were challenged with Ca^{2+}-containing medium (Ca1). The traces shown are the average of 3-6 independent experiments (with 59-144 cells each one). The peak Ca^{2+} signal values (measured as $\Delta F/F_0$; mean ± s.e.m.) were as follows. **A:** Ca1, 1.30 ± 0.30; Ca1+TBH, 6.01 ± 0.24; $p<0.01$. **B:** 6.39 ± 0.58. **C:** 7.39 ± 1.11. B and C were not significantly different but were different from the first stimulus (Ca1) in A ($p<0.01$ and $p<0.001$, respectively).

Fig. 3. Treatment with STIM1 siRNA blocks SOCE. The **e**ffect of siRNA STIM1 [21] on Ca^{2+} entry through plasma membrane was checked by comparing the Ca^{2+} overshoots in transfected and untransfected cells (see text for details). Thapsigargin-treated fura-2-loaded cells perfused with Ca^{2+}-free solution were challenged with medium containing 1 mM Ca^{2+}, as shown. The averaged $[Ca^{2+}]_C$ values of non-transfected cells (control, dotted line) and of cells transfected with STIM1 siRNA plus siGLO OPTI-red (continous line) at the same microscopic field are compared. The $\Delta[Ca^{2+}]$ values were (in nM; mean ± s.e.m.): control, 513 ± 95 (n=10); +STIM1 siRNA, 121 ± 25 (n=16); $p<0.001$.

Fig. 4. Treatment with STIM1 siRNA antagonizes ER Ca^{2+} refilling. Cells expressing ermutGA and reconstituted with coelenterazine n were pre-treated with 10 μM TBH in Ca^{2+}-free solution to empty Ca^{2+} stores. After removing the inhibitor, cells were perfused with a solution containing 1 mM Ca^{2+}, as shown. Control (untransfected) cells, cells transfected with scrambled siRNA and cells transfected with STIM1 siRNA are compared. Each trace is the average of 8 independent experiments. **B.** Bars show quantification of the rate of ER refilling (in μM/s, mean ± s.e.m.): control, 12 ± 0.9; scrambled siRNA, 12.2 ± 0.7; STIM1 siRNA, 3.2 ± 0.1. Difference between control and scrambled siRNA slopes was no significant ($p>0.05$), but STIM1 siRNA caused a 73% inhibition ($p<0.001$).

Fig. 5. Effect of STIM1 siRNA on ER Ca^{2+} refilling in permeabilized cells. Cells were transfected only with ermutGA **(A)** or co-transfected with ermutGA and STIM1 siRNA **(B)** and reconstituted with coelenterazine n. After pre-treatment with 10 µM TBH in a Ca^{2+}-free solution to empty Ca^{2+} stores, the plasma membrane of the cells was permeabilized with 60 µM digitonin for 1 min (DIG) and then perfused with solutions containing [Ca^{2+}] (in nM): 20-500 nM Ca^{2+} (buffered with EGTA) [30]. Traces from representative experiments are shown. **C.** Plot of the rate of ER Ca^{2+} refilling *vs* [Ca^{2+}]. Data from 35 independent measurements are shown.

Fig. 6. Effect of STIM1 siRNA on Ca^{2+} leak from ER and on IP_3-induced Ca^{2+} release. Cells transfected with ermutGA and reconstituted with coelenterazine n were pre-treated with TBH in Ca^{2+}-free as in Fig. 4 and then the intracellular Ca^{2+} stores were allowed to refill by incubation with standard medium containing 1 mM Ca^{2+} (arrow). Then the leak was started either by Ca^{2+} removal (**A**, EGTA) or by stimulation with 100 µM ATP + 100 µM carbachol (**C**, ATP+CCh). Outcomes in control cells, in cells treated with scrambled siRNA and in cells treated with STIM1 siRNA are compared. Each trace is the average of 4 independent experiments. Panels **B** and **D** compare the rates of exit from the ER (mean ± s.e.m.). The differences among the different conditions were not statistically significant.

Fig. 7. Effect of STIM1 siRNA on Ca^{2+} leak from ER and on IP_3-induced Ca^{2+} release in permeabilized cells. Cells pre-treated as in Fig. 6 were permeabilized by digitonin treatment in Ca^{2+}-free solution (DIG). Then the stores were allowed to refill by incubation with a solution containing 100 nM Ca^{2+} (buffered with EGTA; at arrow). At the steady state exit from the ER was forced by Ca^{2+} removal (EGTA arrow; **A.** passive Ca^{2+} leak) or by addition of 5 µM IP_3 (IP_3 bar; **B.**) Each trace corresponds to a representative experiment. **C.** Bars compare the mean values (± s.e.m.; n=4-11) of the rates of Ca^{2+} exit from the ER. The values obtained in control cells and in cells treated with siRNA were not significantly different.

Fig. 8. Effect of STIM1 siRNA on Ca^{2+} release from ER through the RyR. Cells were pre-treated with TBH in Ca^{2+}-free solution as in Fig. 6 and then, cells were perfused with standard medium containing 1 mM Ca^{2+} to refill Ca^{2+} stores for different times. In **A.** exit was induced with different caffeine concentrations (see examples of protocols in supplementary Supplemental Fig. S3) and the rate of Ca^{2+} release for different caffeine concentrations is plotted as a function of the $[Ca^{2+}]_{ER}$ level at the time of caffeine addition. Controls and STIM1 siRNA-treated cells are shown by unfilled and filled symbols, respectively. Data from 30 independent experiments. Traces have been adjusted for every caffeine concentration (circles, 2 mM; triangles, 5 mM; squares, 20 mM; inverted triangles, 50 mM). **B.** Three-dimensional plot summarizes the results of 60 independent experiments with caffeine. Red and cyan balls correspond to intact cells, while blue balls correspond to permeabilized cells.

Fig. 9. Effect of STIM1 siRNA on Ca^{2+} uptake by mitochondria. The kinetics of Ca^{2+} uptake in control and STIM1 siRNA-treated permeabilized cells are compared. Cells were transfected with the low affinity probe mitmutGA, pre-

treated with 10 μM TBH in a calcium-free solution and reconstituted with coelenterazine n. After permeabilization with digitonin in Ca^{2+}-free medium the cells were perfused with intracellular-like solutions containing 2, 5, 10 and 30 μM [Ca^{2+}]. Each point corresponds to mean ± s.e.m. values of a total of 3-6 independent measurements.

SUPPLEMENTAL DATA

Supplemental figures

Supplemental Fig. S1. Treatment with STIM1 siRNA blocks the expression of STIM1. This was confirmed by western blot analysis of control and STIM1 siRNA knockdown cells. Extracts from control (lane 1) and transfected cells (lane 2; 100 nM siRNA) are compared. In three independent determinations the inhibition of STIM1 expression was of (mean ± s.e.m.) 53 ± 5 % ($p<0.01$ against endogenous expression).

Supplemental Fig. S2. Rates of Ca^{2+} exit from the ER in intact and permeabilized cells. A. Ca^{2+} leak induced by Ca^{2+} removal (EGTA) in intact cells. Cells were first allowed to refill ER by adding 1 mM Ca^{2+} (arrow) during 3 min. Note logarithmic scale for $[Ca^{2+}]_{ER}$. **B.** Ca^{2+} leak induced by IP_3-producing agonists (ATP+CCh). Details as in A. Note the existence of two exit phases at different rates. **C.** Comparison of the exit rates induced by Ca^{2+} removal (circles), cyclopiazonic acid (triangles) or agonist stimulation (inverted triangles) in permeabilized cells. Only the release period is shown at expanded time scale. Figures beside the lines correspond to the values first order rate constants (k) calculated from the equation $S_t/S_0 = e^{-k \cdot t}$, where t stands for time (in s) and S_0 and S_t stand for $[Ca^{2+}]_{ER}$ values at time = 0 and time = t.

Supplemental Fig. S3. Ca^{2+} release from ER through the RyR in intact cells. Cells were pre-treated with TBH in Ca^{2+}-free solution as in Fig. 6. Then, cells were perfused with standard medium containing 1 mM Ca^{2+} for different periods, as shown. **A.** Release was induced after reaching the $[Ca^{2+}]_{ER}$ steady state by two consecutive pulses of 5 and 50 mM caffeine (Caf). **B. T**he cells were challenged by two consecutive pulses of 50 mM caffeine at the beginning and at the end of the ER refilling. Each panel illustrates a representative protocol. Other caffeine concentrations were tested similarly. For a summary of results see Fig. 8.

Supplemental Fig. S4. Ca^{2+} release from ER through the ryanodine receptors in digitonin-permeabilized cells. Experiments were performed in cells treated as in supplemental Fig. S3, which were permeabilized with 60 μM digitonin (not shown in the figure) and allowed to refill ER by incubation with 100 nM Ca^{2+} in an intracellular-like solution (arrow). Caffeine was added in two consecutive pulses of 5 and 50 mM. Each trace shows a representative result. Other $[Ca^{2+}]_{ER}$ levels were obtained by changing $[Ca^{2+}]_C$ during refilling. Caffeine concentrations of 2 and 20 mM were also tested. For a summary of results see Fig. 8B.

Supplemental Fig. S5. Effect of STIM1 siRNA on Ca^{2+} uptake by mitochondria. Cells were transfected with mitGA and pre-treated with 1 μM thapsigargin in Ca^{2+}-free solution to empty Ca^{2+} stores. At the time shown by the arrow 5 mM Ca^{2+} was added. mitAEQ was reconstituted with native coelenterazine. The lines correspond to averaged traces of 9-11 individual experiments. The $\Delta[Ca^{2+}]$ values were (in μM; mean ± s.e.m.): 2.88 ± 0.08 for control cells and 1.46 ± 0.13 for the STIM1 siRNA-transfected cells. The

difference was significant ($p<0.001$). For results in permeabilized cells see Fig. 9.

Supplemental Fig. S6. Effects of STIM1 siRNA on the ER-mitochondria interaction. Cells were transfected with mitGA and reconstituted with native coelenterazine in the presence of 1 mM Ca^{2+}. Then, Ca^{2+} release from the ER was induced by **A.,** 100 μM ATP, **B.,** 100 μM carbachol (CCh) or **C.,** 5 mM caffeine (Caf); in this last case cells were co-transfected with the RyR2 cDNA. Each trace is the average of 3-4 experiments. The differences of the $\Delta[Ca^{2+}]$ values were not significant.

Supplemental Fig. S7. Effects of STIM1 siRNA on the Ca^{2+} entry into the nucleus. Cells were transfected with nucGA and reconstituted with native coelenterazine in the presence of 1 mM Ca^{2+}. Ca^{2+} release from ER was induced by perfusing with 100 μM ATP. Each line is the averaged value of 4 experiments. The differences of the $\Delta[Ca^{2+}]$ values were not significant.

Fig. 1

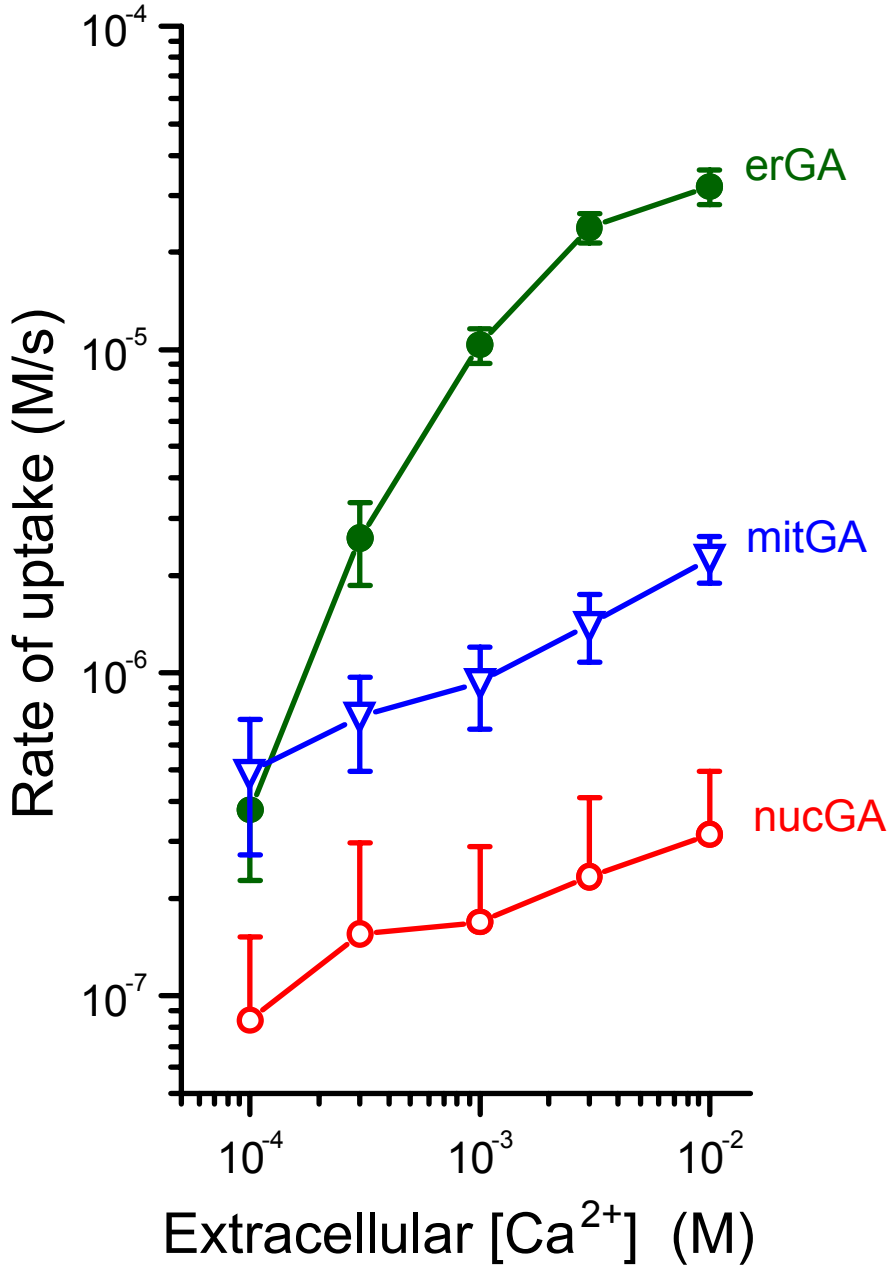
Rate of uptake (M/s)
10-4
10-5
10-6
10-7
erGA
mitGA
nucGA
10-4
10-3
10-2
Extracellular [Ca2+] (M)

Fig. 2

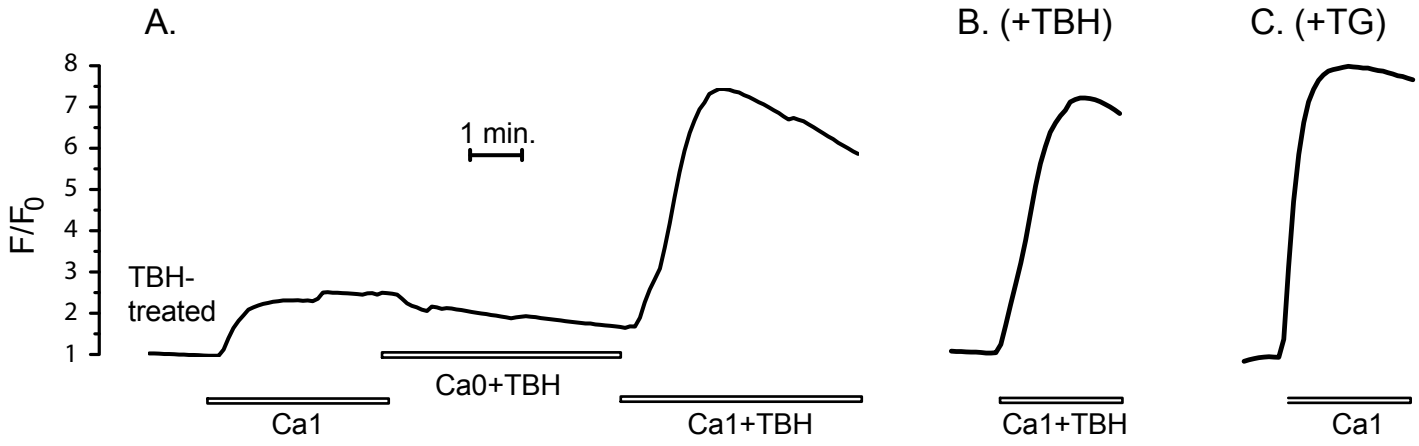
A.
B. (+TBH)
C. (+TG)
F/F0
8
7
6
5
4
3
2
1
1 min.
TBH-
treated
Ca1
Ca0+TBH
Ca1+TBH
Ca1+TBH
Ca1

Fig. 3

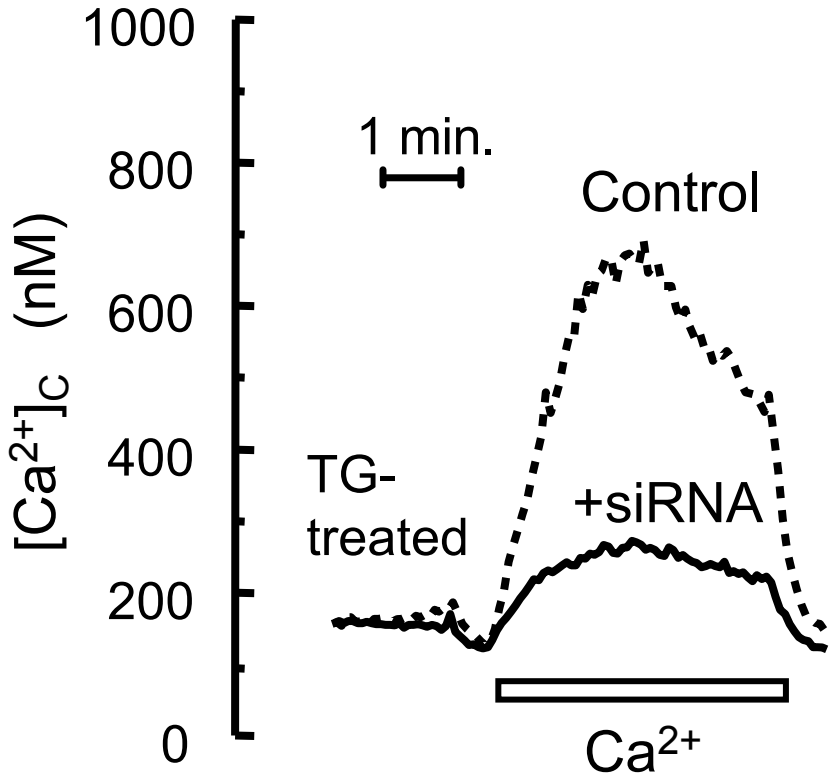
1000
800
600
400
200
0
[Ca2+]C (nM)
1 min.
Control
TG-
treated
+siRNA
Ca2+

Fig. 4

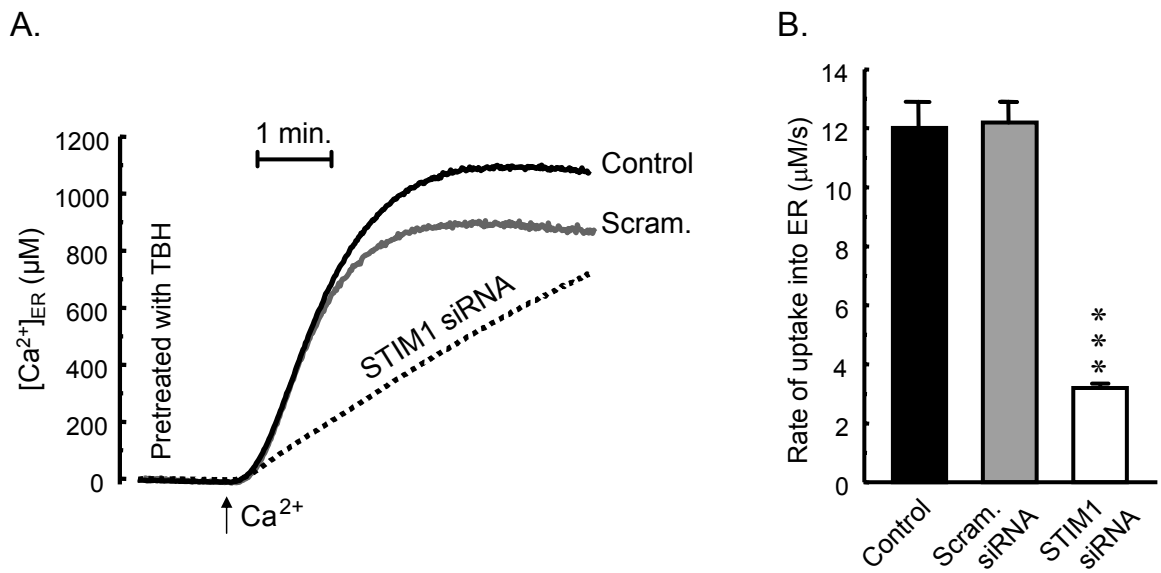
A.
1 min.
Control
Scram.
STIM1 siRNA
Pretreated with TBH
$[Ca^{2+}]_{ER}$ (μM)
1200
1000
800
600
400
200
0
Ca^{2+}
B.
Rate of uptake into ER (μM/s)
14
12
10
8
6
4
2
0
***
Control
Scram. siRNA
STIM1 siRNA

Fig 5

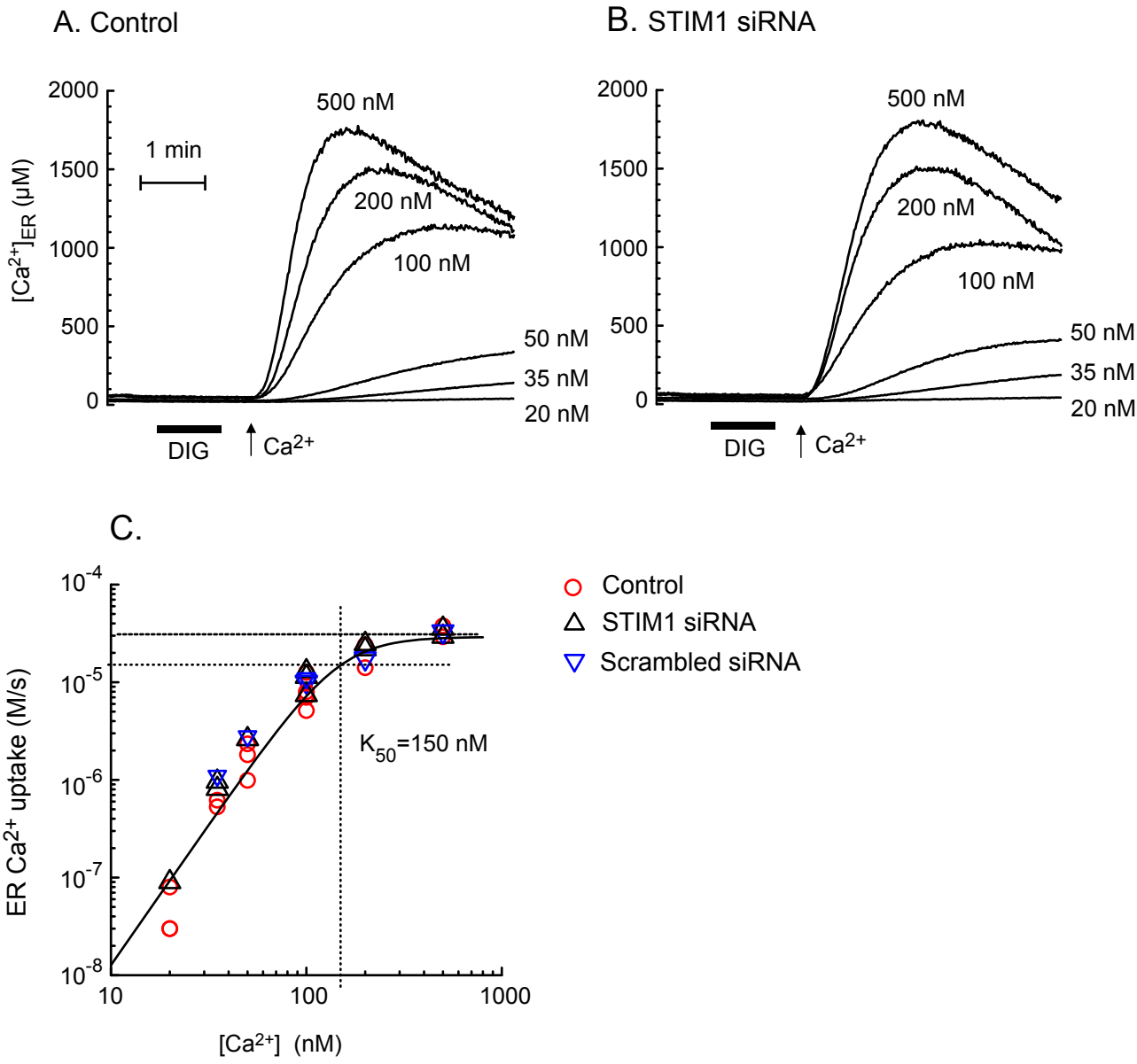
A. Control
B. STIM1 siRNA
2000
1500
1000
500
0
[Ca2+]ER (μM)
1 min
500 nM
200 nM
100 nM
50 nM
35 nM
20 nM
DIG
Ca2+
C.
ER Ca2+ uptake (M/s)
10-4
10-5
10-6
10-7
10-8
10
100
1000
[Ca2+] (nM)
K50=150 nM
Control
STIM1 siRNA
Scrambled siRNA

Fig. 6

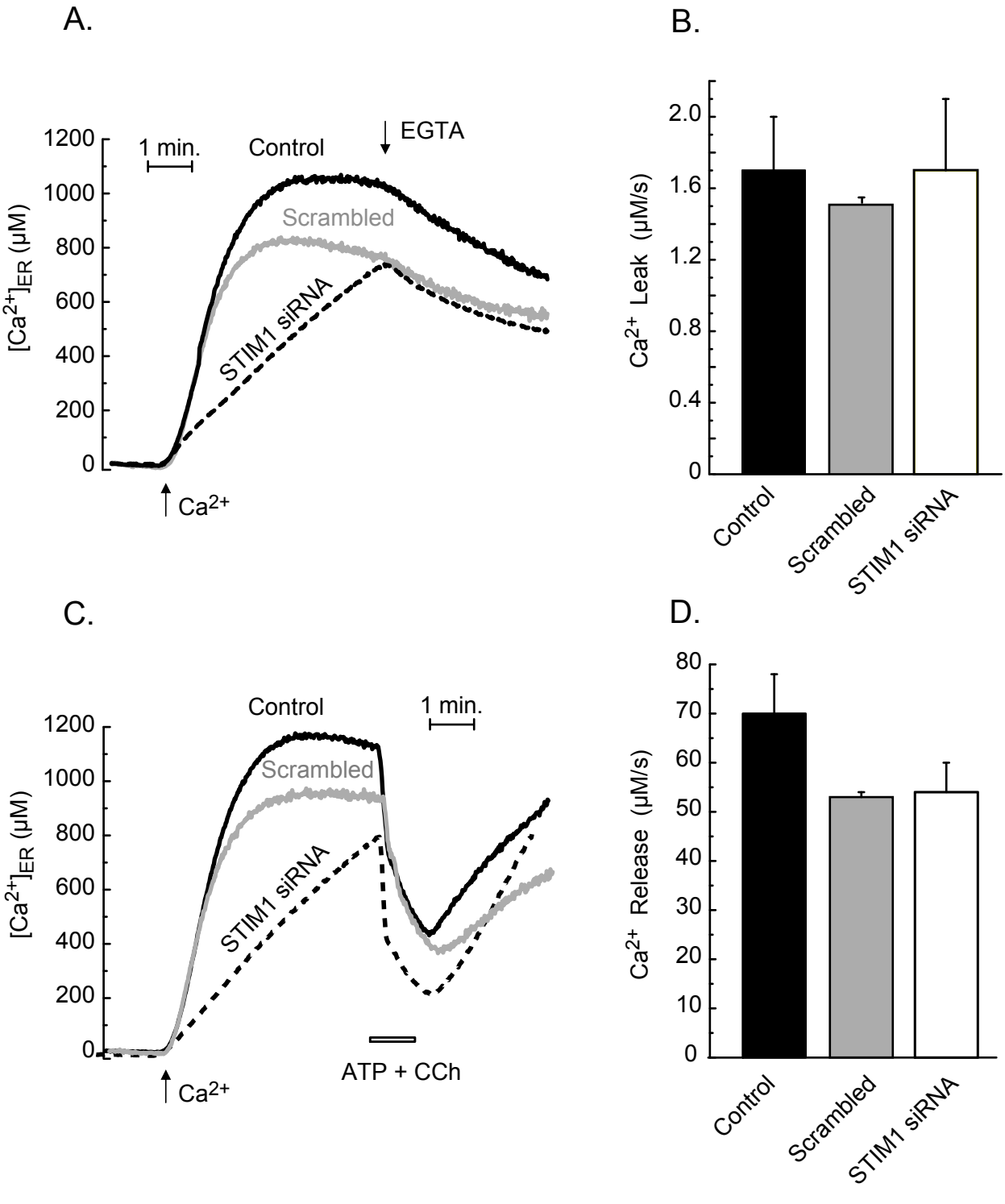
A.
1 min.
Control
EGTA
Scrambled
STIM1 siRNA
Ca2+
[Ca2+]ER (μM)
1200
1000
800
600
400
200
0
B.
Ca2+ Leak (μM/s)
2.0
1.6
1.2
0.8
0.4
0
Control
Scrambled
STIM1 siRNA
C.
Control
1 min.
Scrambled
STIM1 siRNA
Ca2+
ATP + CCh
[Ca2+]ER (μM)
D.
Ca2+ Release (μM/s)
80
70
60
50
40
30
20
10
0
Control
Scrambled
STIM1 siRNA

Fig. 7

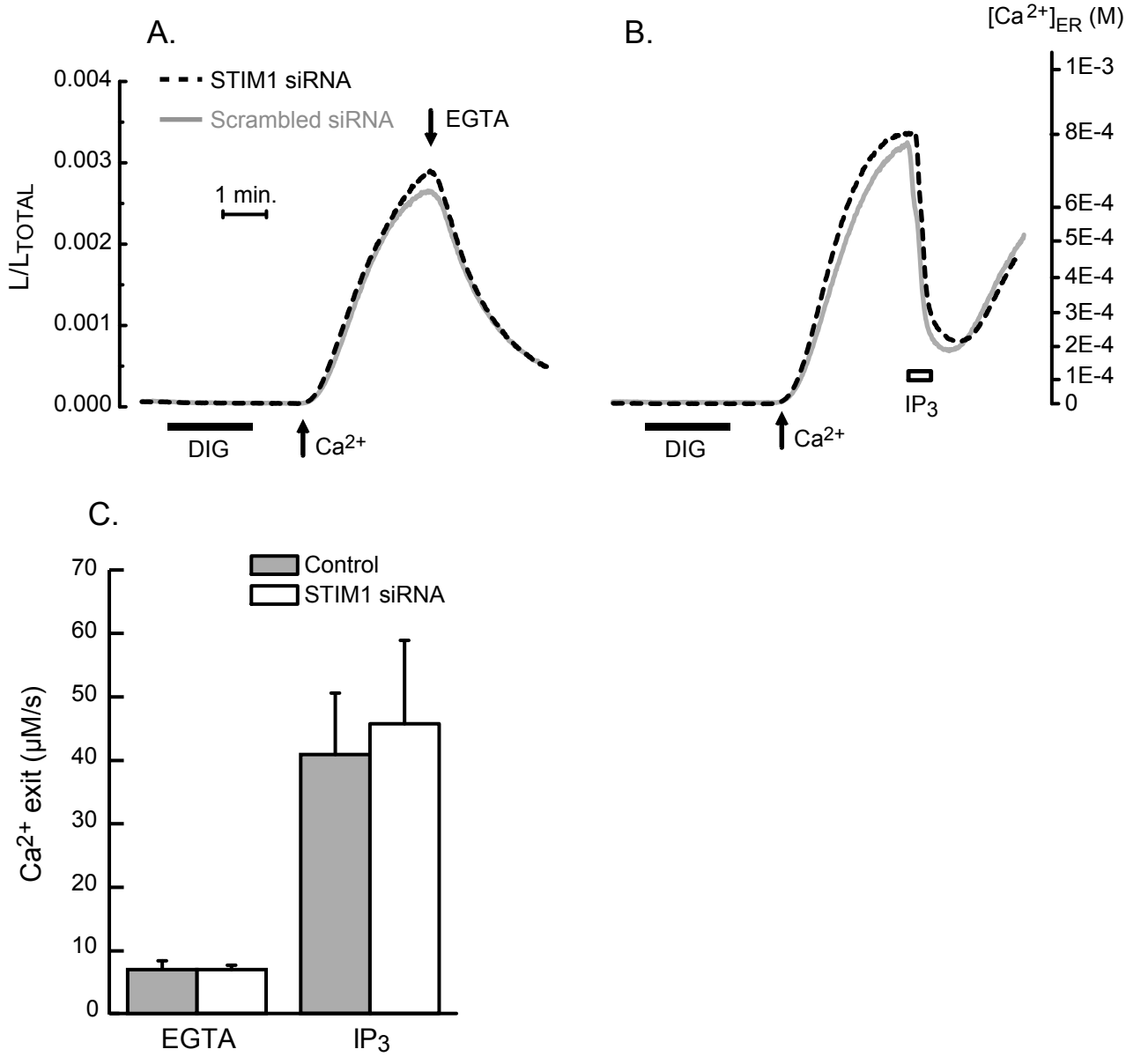
A.
B.
C.
STIM1 siRNA
Scrambled siRNA
EGTA
1 min.
DIG
Ca2+
IP3
L/LTOTAL
[Ca2+]ER (M)
Control
STIM1 siRNA
Ca2+ exit (μM/s)
EGTA
IP3

Fig. 8

A.

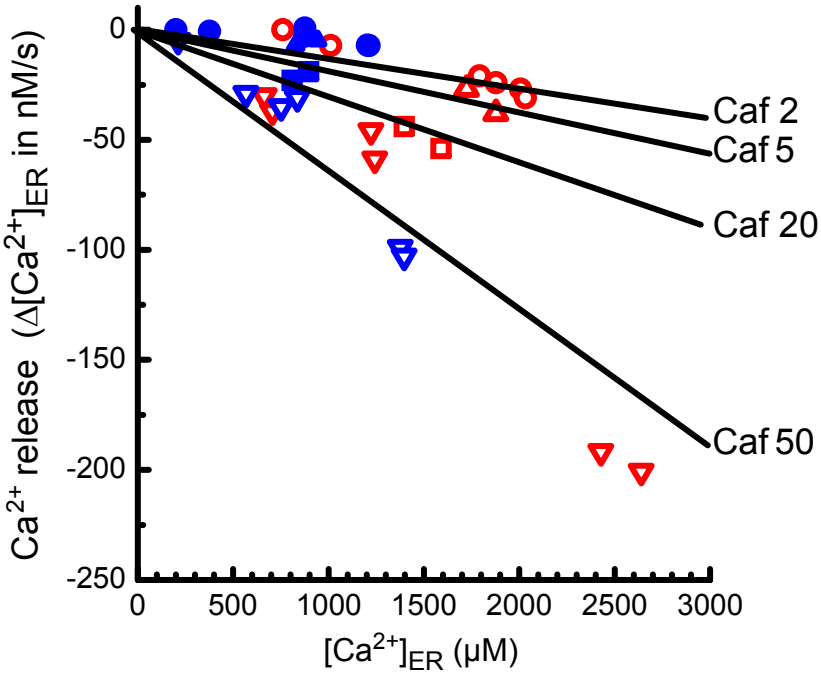
0
-50
-100
-150
-200
-250
0
500
1000
1500
2000
2500
3000
Ca2+ release (Δ[Ca2+]ER in nM/s)
[Ca2+]ER (μM)
Caf 2
Caf 5
Caf 20
Caf 50

B.

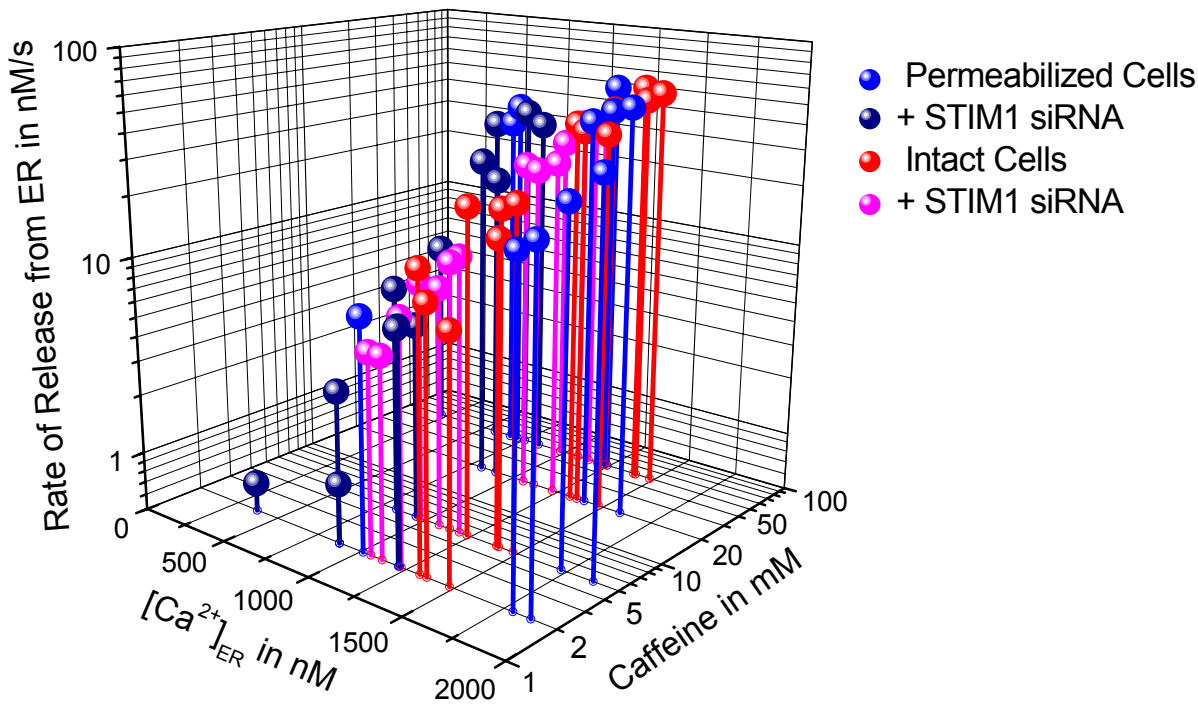
Rate of Release from ER in nM/s
100
10
1
0
500
1000
1500
2000
[Ca2+]ER in nM
1
2
5
10
20
50
100
Caffeine in mM
Permeabilized Cells
+ STIM1 siRNA
Intact Cells
+ STIM1 siRNA

Fig.9

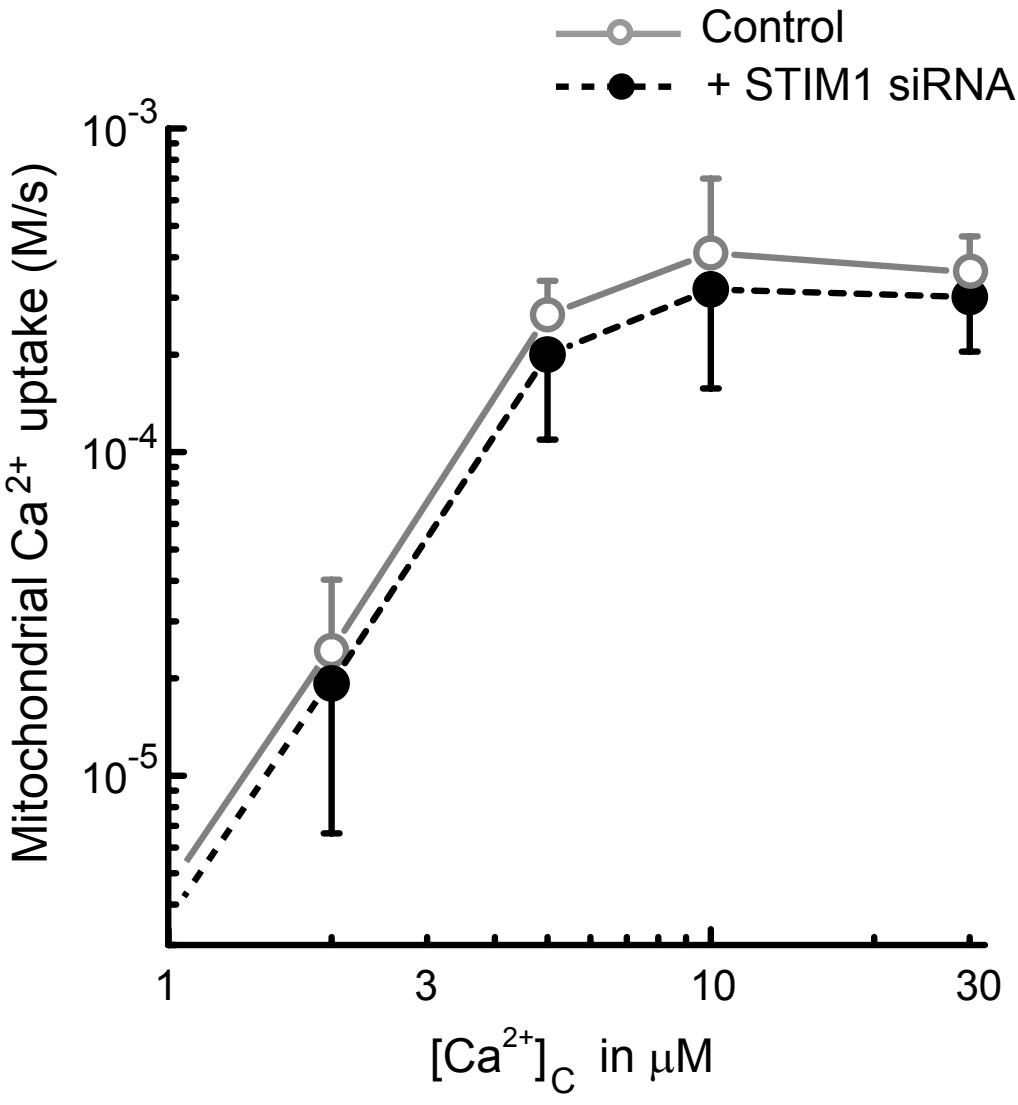
Control
+ STIM1 siRNA
Mitochondrial Ca2+ uptake (M/s)
10-3
10-4
10-5
1
3
10
30
[Ca2+]C in μM

Supplemental Fig. S1

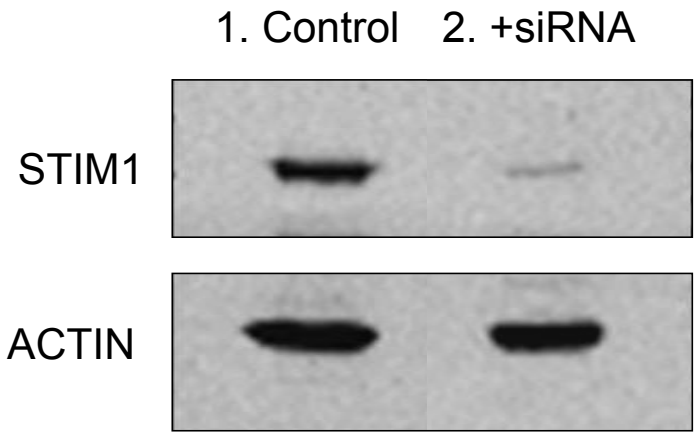

Supplemental Fig. S2

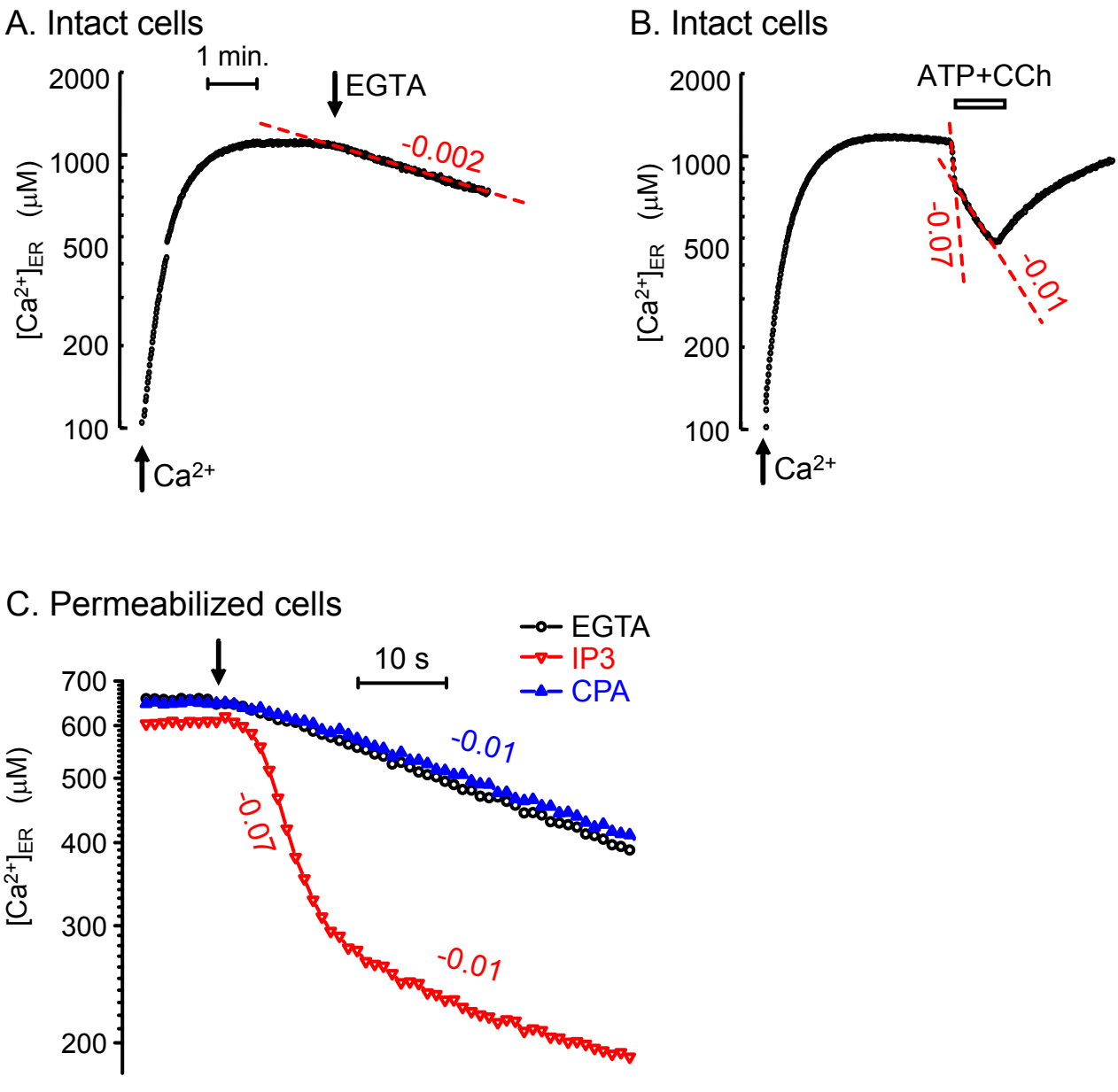

Supplemental Fig. S3

A.

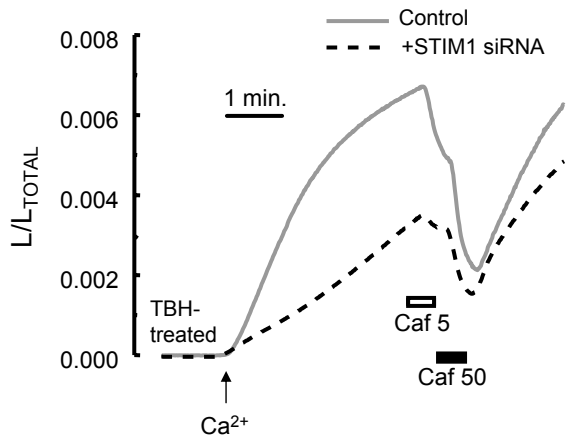

B.

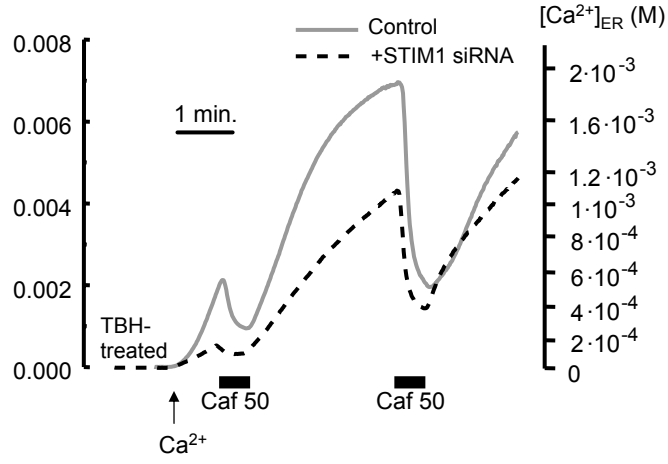

Supplemental Fig. S4

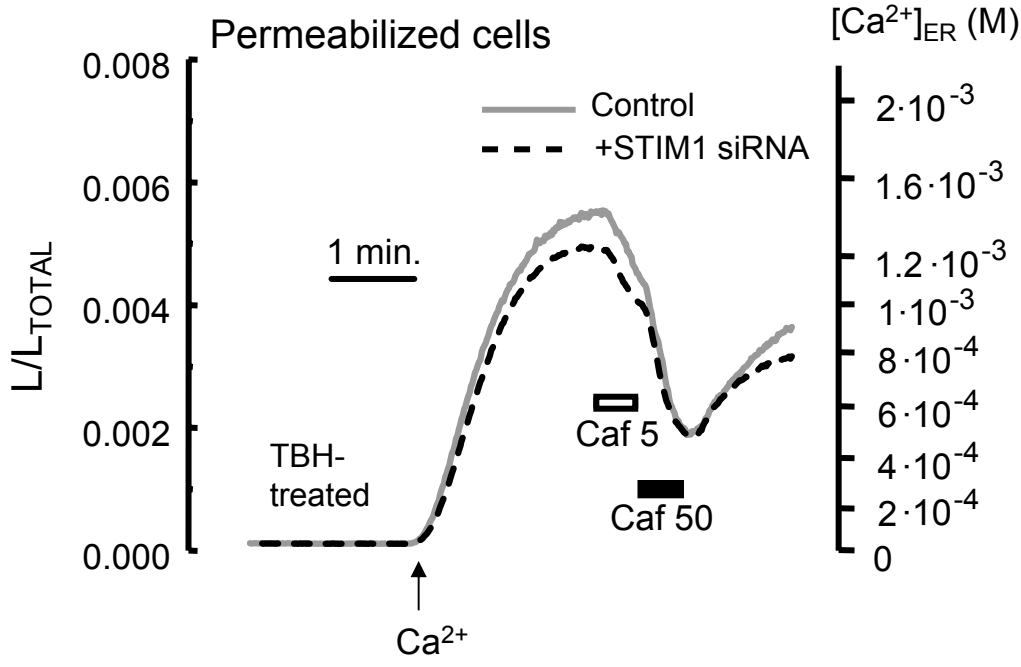

Supplementary Fig. S5

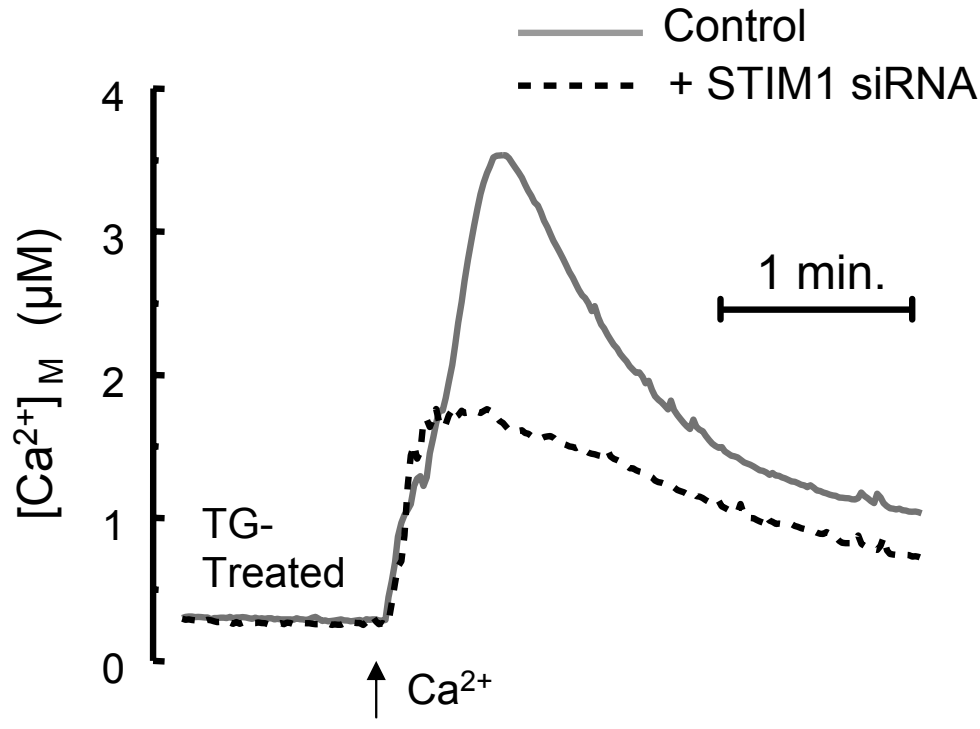

Supplementary Fig S6

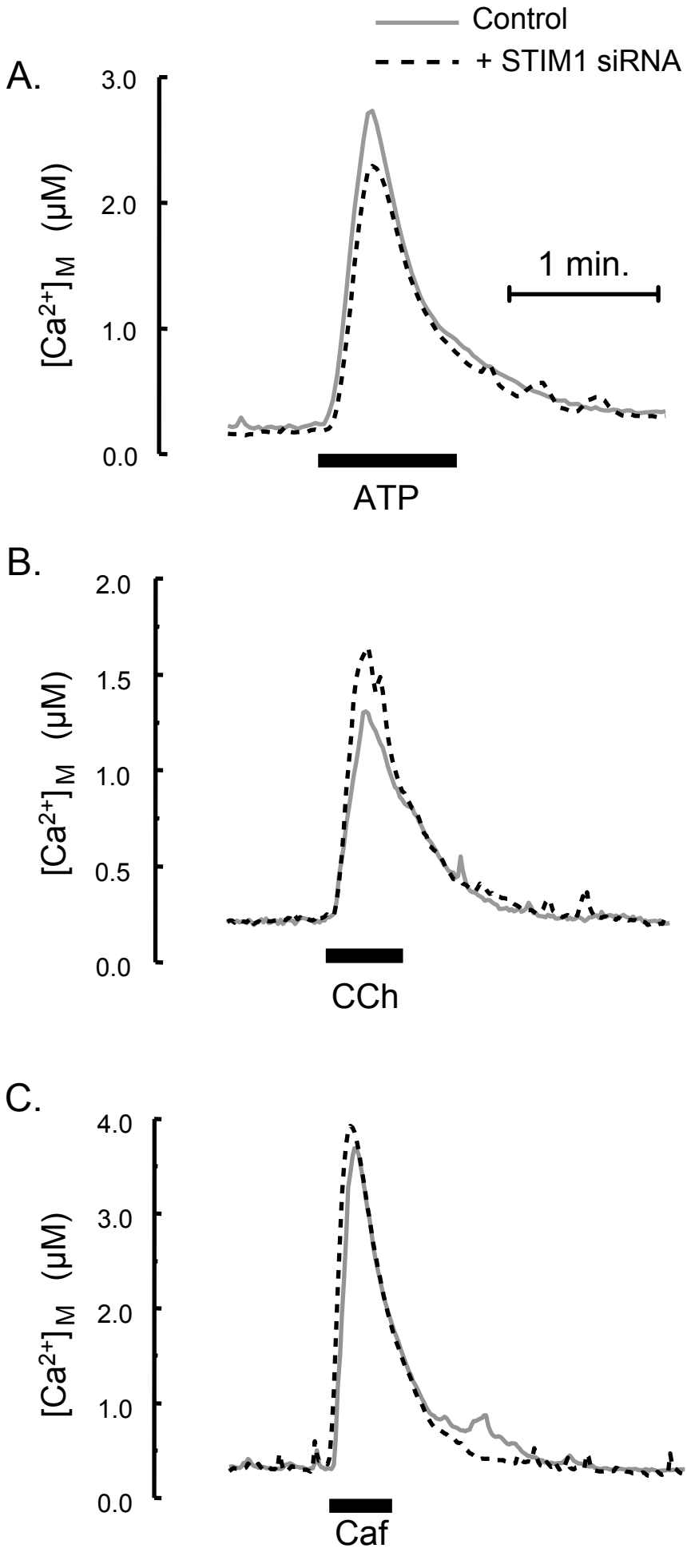

Supplementary Fig. S7